PYROCLASTIC EVIDENCE OF SYN-ERUPTIVE DEGASSING AT THE EXPLOSIVE/EFFUSIVE TRANSITION

by

EMILY SUZANNE MATTHEWS

KIMBERLY GENAREAU, COMMITTEE CHAIR

RONA DONAHOE
JOSEF DUFEK
HAROLD STOWELL

A THESIS

Submitted in partial fulfillment of the requirements
for the degree of Master of Science in the
Department of Geology in the Graduate School
of The University of Alabama

TUSCALOOSA, ALABAMA

2016

ABSTRACT

The 2010 eruption of Merapi (Java, Indonesia) initiated with an uncharacteristic explosion, followed by rapid lava dome growth and collapse, all of which generated deadly pyroclastic density currents (PDCs). PDC samples from the initial explosion on October 26th were collected from several locations surrounding the edifice. Plagioclase phenocrysts represent the primary component of the dominant ash mode due to the elutriation of the finer ash fraction during PDC transport. Secondary electron images of 45 phenocrysts were taken using the scanning electron microscope (SEM) to examine preserved glass coatings on phenocrysts, which represent the interstitial melt within the magma at the point of fragmentation. Using these images, the bubble number densities (BNDs) were determined, and the decompression rate meter of Toramaru (2006) was used to calculate the decompression rate during the initial explosion of the 2010 Merapi eruption. Calculated decompression rates range from 6.08×10^7 Pa/s to 1.4×10^8 Pa/s. Decompression rates have shown to correlate with eruption column height; therefore Merapi's rates should be similar to those of other Vulcanian explosions, because the eruption column was 8-9 km in height. Sakurajima volcano (Japan) experienced decompression rates from 7.0×10^3 to 7.8×10^4 Pa/s during the later phase of the fall 2011 Vulcanian explosions. Plinian explosions, such as at the 1991 eruption of Mt. Pinatubo and the 1980 eruption of St. Helens had much higher column heights compared to the initial 2010 Merapi explosion; 35 km, 19 km, and 8-9 km, respectively, but decompression rates in a comparative range (10^8 Pa/s). Higher decompression rates during the 2010 initial explosion at Merapi likely resulted from

increased overpressure in the shallow conduit, as revealed through previous geochemical analyses of the erupted crystals Results indicate that decompression rates may be underestimated for Vulcanian explosions.

LIST OF ABBREVIATIONS AND SYMBOLS

SEM Scanning electron microscope

BND Bubble number density

PDC Pyroclastic density current

Wt% Weight percent

DR Decompression rate

SIMS Secondary ion mass spectroscopy

ACKNOWLEDGMENTS

My biggest thanks goes to Dr. Genareau, my advisor and committee chair, for sharing her research expertise and for providing a listening ear throughout this process. I would also like to thank all of my committee members, Dr. Rona Donahoe, Dr. Josef Dufek, and Dr. Harold Stowell for their invaluable input, inspiring questions, and support of both my thesis project and my academic progress. Being surrounded by some of the smartest and most experienced minds in geology has really pushed me and inspired me the past two years. Also, a huge thanks to NSF EAR1358886 funding for their contribution to this project.

It was a struggle mentally and emotionally when I began graduate school with the quick passing of my grandmother after a cancer diagnosis while also planning my wedding. I was worn down, but with the help of my advisor and lab mates, I pushed though and am able to prepare for graduation, job searching, and the birth of my daughter.

This research would not have been possible without the support of my friends and fellow graduate students and of course of my husband and parents who never stopped encouraging me to push through the exhaustion. I wouldn't be here without them.

CONTENTS

LIST OF TABLES

LIST OF FIGURES

1

INTRODUCTION

Volcanic eruptions are one of the Earth's most dangerous natural processes that may result in loss of lives and infrastructure. Volatiles in the melt can have a large effect on eruption style and the destructive nature of the eruption. Magma stored in a magma chamber contains dissolved volatiles, with the most prominent being H_2O. Others, such as CO_2 and SO_2, are also present but in smaller amounts (Figure 1)(Scandone et al., 2007). However, these volatiles are just as important in eruption dynamics as well as long-term climate change after an eruption (Wallace et al., 1995, Gonnermann and Manga, 2007). Andesitic volcanism typically has viscous magma due to the silica content and large amount of volatiles within the system.

Effusive activity is common at most andesitic volcanoes, where the volatiles within the melt are able to escape through efficient degassing of the lava (Hammer et al., 2000; Sparks, 2003; Shinohara, 2008). Effusive eruptions are nonexplosive discharges of magma to the surface to form lava flows and domes, and are caused by volatiles being exsolved and moving out of the magma into the volcanic conduit walls or escaping through the vent during ascent (Nguyen et al, 2014; Sparks et al., 2003; Preece et al., 2014). Fragmentation is a process by which magma transitions from a melt phase with bubbles and mineral crystals into pieces of tephra surrounded by a gas phase (Alidibirov and Dingwell, 1996; Wallace et al., 1995; Gonnermann and Manga, 2007; Gonnermann, 2015). Explosive eruptions will occur if the

viscous magma cannot efficiently degas during rapid magma ascent, building overpressure in the system. As magma begins to ascend through the conduit from the chamber at depth, the dissolved volatiles become oversaturated and bubbles nucleate (Sparks, 1978; Toramaru, 1989; Proussevitch et al., 1993; Sparks et al., 1994; Toramaru, 1995; Proussevitch and Sahagian, 1996; 1998; Jaupart, 1996; Cashman, 2004). The acceleration created by the formation and growth of bubbles then creates a driving force for a volcanic eruption. Due to the high viscosity of intermediate magmas typical at active stratovolcanoes, equilibrium bubble growth is impeded during magma ascent, resulting in the development of overpressure within the bubbles.During explosive eruptions, bubbles will burst as a result of overpressure and cause fragmentation of the magma following sudden decompression. The open-system degassing characteristic of an effusive eruption results in the loss of a fragmentation surface necessary for explosive eruptions. Andesitic stratovolcanoes typically cycle between both styles of activity.

Vulcanian explosions are discrete, short-lived events that produce magma columns up to 20 km in height. Plinian explosions are sustained events that can last hours to days, producing column heights in excess of 20 km (Klug and Cashman, 1994). Bubble nucleation regimes vary between these two eruption styles, as homogeneous nucleation of bubbles is typical during Plinian eruptions due to the high decompression rate ($>10^8$ Pa/s) (Toramaru, 2006). This is due to the melt being so oversaturated with volatiles that bubbles spontaneously form directly in the melt. In heterogeneous nucleation, the bubbles nucleate on crystal surfaces (Hurwitz and Navon, 1994; Gardner and Denis, 2004; Gardner, 2007; Cluzel et al., 2008). Heterogeneous nucleation is

more common in explosions with decompression rates comparable to those observed at similar Vulcanian events (Sakurajima volcano, Japan) using extension cracks in crystals from pumice samples (10^3-10^4 Pa/s) (Miwa and Geshi, 2012). The extension-cracked crystals are created by vesiculation of magma (Kennedy et al., 2005). In order to calculate decompression rate of magma during crack formation, Miwa and Geshi (2012) modeled the time duration and the amount of decompression occurring during the opening of the crack.

The purpose of this study is to determine if decompression rates of Vulcanian eruptions may be underestimated in some cases or if nucleation dynamics during Vulcanian events may be affected through preferential nucleation of bubbles on crystal surfaces in viscous andesite magmas.

a. Field Area

Gunung Merapi is located in the Sunda arc region of Indonesia that formed by the subduction of the Indo-Australian Plate beneath the Eurasian Plate (Figure 2) (Hamilton, 1979). This subduction zone creates a large amount of island-arc volcanism on Indonesia, and Merapi is considered one of the most active and dangerous stratovolcanoes in the region (Gertisser et al., 2012). Over the past two centuries, Merapi's activity has been dominated by periods of andesitic dome growth and dome failure that has produced pyroclastic density currents every few years (Voight et al., 2000). The 2006 event, the most recent before 2010, experienced typical extrusive eruptive behavior with dome growth and gravitational collapse (Holland et al., 2011; Charbonnier and Gertisser, 2008; Charbonnier and Gertisser, 2009; Lube et al., 2011). The

andesite dome erupted in 2006 remained until the fall of 2010 when Gunung Merapi had a multi-phase eruption that was fueled by pressurized volatiles (Table 1). Phase 1, known as the 'intrusion phase' was characterized by increased seismicity and inflation of the volcanic edifice (Surono et al., 2012) due to protracted degassing of juvenile magma beneath the pre-existing 2006 lava dome. These precursors, such as edifice inflation, volcanic tremors, and volcanic gas emissions were typical of prior activity, suggesting that any potential eruption would be similar to others, which usually began by dome collapse and more effusive, non-explosive events (Surono et al., 2012). However, on 26 October 2010, Merapi erupted explosively after two months of observed seismic activity and ground deformation. The 26 October Vulcanian explosion was considered phase 2 of the eruption, and produced a column 8-9 km in height, cleared the volcanic vent of the pre-existing lava dome, and resulted in the formation of pyroclastic density currents (PDCs). These currents are composed of high temperature gases containing ash and other volcanic debris that can travel for several kilometers.

The overpressure that developed in the shallow plumbing system during phase 1 resulted in brittle failure of the pre-existing lava dome and decompressed the system, causing nucleation and rapid growth of bubbles in the melt phase of the magma, which accelerated magma ascent until the fragmentation surface was reached. This allowed the formation of pyroclasts in the form of ash (< 2 mm), containing crystals, and lava lapilli (2-64 mm). An effusive eruption followed the initial explosion and was considered phase 3. This effusive eruption culminated on 5 November 2010 with collapse of the lava dome, which generated a large PDC that reached ~22

km from the summit (Charbonnier et al., 2013). This phase of the eruption was very destructive, and killed over 300 people in the path of the PDCs. Low intensity activity, such as rock falls and small pyroclastic flows, continued throughout November, and in early December, the alert level was lowered from 4 to 3 (on a scale of 1-4) (Gertisser et al., 2011).

Previous research (Toramaru, 2006) on pumice lapilli from Plinian eruptions determined that magma decompression rates (Pa/s) could be calculated using preserved vesicles, or the bubble number density (BND), of pumice. The decompression rate quantifies how quickly the overpressure is released during an explosive volcanic eruption. Plinian eruptions, like the 1980 Mount St. Helens eruption, typically have much greater column heights than Merapi's 2006 event (24 km vs 8-9 km, respectively)(Blundy and Cashman, 2001; Blundy and Cashman, 2005). This results from overpressure within the conduit, sudden decompression, and efficient magma fragmentation. Toramaru's decompression rate meter uses the BND for each sample and magmatic properties (e.g., temperature, H_2O diffusivity) to calculate decompression rate at the point of eruption and fragmentation. Toramaru (2006) states that a positive correlation exists between decompression rate and column height, whereby the higher rate of decompression produces a higher column height. According to the correlation found by Toramaru (2006) between column height and decompression rate, the Merapi magma should have experienced a decompression rate similar to other Vulcanian style eruptions (10^4 Pa/s), as the observed column height ranged between 8-9 km. Determining the decompression rate during the initial explosion, and comparing this value to other Vulcanian events could give insight into the degassing dynamics occurring within the conduit, and potentially explain the uncharacteristic nature of the

2010 eruption. For the Merapi 2010 explosion, it was hypothesized that the rates would be higher due to evidence of overpressure development (Genareau et al., 2014) in the magma prior to the sudden decompression event. The method of calculating BND on crystal surfaces used in this study to calculate the magma decompression rate is new and novel, and may be useful for the analysis of explosive deposits in future studies.

2

METHODOLOGY

a. Previous work

Previously acquired data (Genareau et al., 2014) from Secondary Ion Mass Spectrometer (SIMS) depth profiles of the same plagioclase phenocrysts utilized in this study were examined to analyze the behavior of rapidly diffusing elements (Li and H) within the phenocrysts during the final stages of ascent. Previous depth-profiling studies (Genareau et al., 2009; Genareau and Clark, 2010) suggest that Li could indicate degassing of volatiles during magma ascent. The behavior and build-up of Li in the phase 2 crystal glass groundmass showed that the volatiles exsolving from the melt were accumulating in the shallow conduit and contributed to the overpressure development prior to the eruption. In contrast, depth profiles of phase 3 crystal groundmass showed an efficient loss of Li from the melt due the higher rate of volatile diffusion (Genareau et al., 2014). This, coupled with greater amount of microlites on the crystal surfaces, indicates more efficient degassing during this phase, causing the Li to escape more rapidly.

The plagioclase phenocrysts represent an efficiently fragmented portion of the magma in the phase 2 PDC deposits. Evidence is shown in phase 2 ash, which is dominated by crystals, while phase 3 is dominantly lava. The JEOL JSM-6010PLUS/LA InTouchScope scanning electron microscope (SEM) at the University of Alabama Tephra Lab was used to image glass

adhering to crystal surfaces (Figure 4) in secondary electron mode in order to quantify bubble number density, the percentage of connected vesicles, and directionality of vesicles at the point of fragmentation during the eruption. In order to calculate decompression rate, only the phase 2 crystals were used because these represent the state of magma vesiculation during the initial explosion of 26 October when rapid decompression occurred.

b. Approach

The secondary electron images of crystals were analyzed using ImageJ freeware (http://imagej.nih.gov/ij/). By measuring the area of each crystal face, counting the number of bubbles on the crystal surface, and measuring an average bubble diameter, bubble number density (BND) was calculated using the following equation. **Equation 1**:

$$BND = N_A/D$$

Where N_A is the number density per unit area and D is the average bubble diameter. The BND (m^{-3}) is controlled by physical properties of the magma (e.g., H_2O diffusivity, viscosity, temperature) that influence the extent of vesiculation. The BND decompression rate meter (Toramaru, 2006) determines decompression rate (Pa/s) using the calculated BND and melt properties (Table 2). The variables for this equation were either calculated using equations in Toramaru (2006) or were found in previous studies on Merapi's system. The most important melt factors included Si content (wt%), melt temperature (K), and H_2O wt%. All of these can vary by volcano based on their magma composition, and can vary by eruption if there are

changes in volatile concentration. Petrological studies (Costa et al., 2013) on the 2010 Merapi eruption products were used to accurately characterize the melt and give insights to the magma storage conditions and processes.

In this study, bubble number densities were calculated using glass adhering to plagioclase crystal surfaces that had well-preserved vesicles (Figure 4). The crystals with a low number of easily identifiable bubbles walls and high number of microlites were shown to be crystals from phase 3 where efficient degassing occurred (Cichy et al., 2011; Genareau et al., 2014), and were not included in the measurements. The decompression rate was then determined using Equation 2.

Equation 2: Decompression rate (Pa/s)

$$= a \cdot D \cdot \delta^2 \cdot Pw^{-1/3} \cdot T^{-1/2} \cdot N^{2/3}$$

Where a is a constant ($1x10^{15}$), D is diffusivity of water (m^2/s), δ is interfacial tension (N/m) as a function of T and P_w, P_w is initial saturation pressure (Pa), T is melt temperature (K), and N is bubble number density (m^{-3}).

Once the decompression rates were calculated, a sensitivity analysis was run to determine how the rates would change if the properties of the melt varied. Due to the uncharacteristic nature of this particular eruption, it is important to understand what property, or properties, of the melt may have altered the bubble nucleation dynamics, or if magma-water interactions influenced the nucleation dynamics. The temperature was varied by 100 K increments from 800-

1400 K. This range accounts for variations in crustal assimilation, H_2O wt% and volatile saturation in petrological samples from the 2010 eruption (Costa et al., 2013).

Diffusivity of water (m^2/s) is functions of melt temperature, SiO_2 content, H_2O content, and pressure. Therefore, understanding changes in these characteristics of the melt was essential in determining how much the H_2O diffusivity may vary. The diffusivity range used for this calculation was interpreted from Toramaru (2006) as a function of wt% SiO_2. The interfacial tension was recalculated with changes in temperature and saturation pressure using Equation 3.

Equation 3: Interfacial tension

$$= 0.2366\exp\left(\left((-0.35 * 10^{-6}) \cdot Pw - (11 * 10^{3})\left(\frac{1}{T} - \frac{1}{1273}\right)\right)/\mathrm{R}\right)$$

Where P_w is initial saturation pressure (Pa), T is melt temperature (K), and R is a gas constant (8.3 J/K). Saturation pressure in the sensitivity analysis was contained within a range ($1x10^8$ – $2x10^8$ Pa) that was found in previous studies on Merapi/andesitic magma and related to silica content (Costa et al., 2013). The newly calculated values were plotted against the original rates to determine what parameters caused the 2010 Merapi decompression rates to be significantly different than other Vulcanian-style eruptions around the world.

Using the correlation between column height and decompression rate (Toramaru, 2006), an equation was used to calculate the expected column height (Equation 4) (Figure 5).

Equation 4: Column height (km)= $0.0681 \cdot (DR^{0.0031})$

Where DR= calculated decompression rate.

3

RESULTS

The calculated BND varied by crystal ($1x10^{13}$ to $4x10^{12}$ m^{-3}) with crystal size, bubble number, bubble diameter, etc. After determining the BND in order to calculate the decompression rate of phase 2 using the decompression rate meter (Toramaru, 2006) (Table 3, Table 4), it was necessary to compare the numbers in order to confirm or deny the hypothesis that the 2010 Merapi magma experienced a decompression rate higher than those typical of Vulcanian explosions. According to the results, Merapi's decompression rates were significantly higher than expected, and had rates similar to those estimated for much larger volcanic events with column heights 3 or 4 times greater. Using equation 4, Merapi's decompression rates would produce a 25 km-high eruption column. This indicates that the amount of overpressure created by: 1) the plugging lava dome effused in 2006; 2) the juvenile magma ascending from depth; 3) the accumulation of volatiles exsolving from the juvenile magma or 4) magma-water interaction; resulted in a decompression rate typical of a larger Plinian eruption when the 26 October explosion occurred.

Sensitivity analyses were conducted to determine what variables of the decompression rate meter would provide values in a comparable range to other Vulcanian eruptions. Possibilities include a difference in temperature, a greater amount of H_2O in the melt, or a higher saturation pressure. By lowering the temperature by 100 K increments and keeping the other parameters

constant, there was an order of magnitude change (highest rate ~1.23×10^7 Pa/s) but the decompression rate did not approach those comparable to Vulcanian-style decompression rates (10^4 Pa/S) (Figure 6). H_2O content is another factor. A higher amount of H_2O in the melt could create a greater number of bubbles, affecting the measured BND. To examine the effect on the decompression rate, the diffusivity was changed to account for a higher content of SiO_2 (55 wt%- 60 wt%) (Figure 7). The higher the amount of water in the magma, the faster the diffusivity. Saturation pressure is the point at which the magma is completely saturated with volatiles. This is also a factor of water content; therefore this was raised from 3 to 5 wt% H_2O in the sensitivity analysis in order to account for higher H_2O contents (Figure 8).

None of the parameters affected the calculated decompression rates enough to be considered the controlling factor in this explosion. The highest rate calculated by altering the variables was 1.39×10^8 Pa/s, and the lowest rate calculated was 2.65×10^7 Pa/s, three orders of magnitude greater than the typical Vulcanian decompression rate. This suggests that the bubble number density calculated from the plagioclase crystal surfaces provides an accurate representation of vesiculation dynamics during the 2010 initial explosion (Figure 9).

4

DISCUSSION

The plagioclase crystals from the ash component of the 2010 PDCs revealed differences in amount of preserved bubbles and microlite nucleation, which indicates that there were rapid changes in degassing dynamics within the eruptive time frame (Couch et al., 2003). Examining the preservation of bubbles in the glass on the crystal surface and the formation of microlites showed that the degassing dynamics evolved from a closed-system to open-system state during the transition from explosive (phase 2) to effusive (phase 3) activity. The magma from phase 2 was supersaturated with volatiles that were able to nucleate and form bubbles as magma ascended the conduit towards the vent. This phase underwent closed-system degassing, therefore these volatiles were not able to escape through the conduit walls or through the vent, and fragmented bubble imprints were preserved in the glass quenched on the crystal surfaces at the point of fragmentation when the 2006 dome failed collapsed, and the pressure was suddenly released. This caused the bubbles formed by ascent driven decompression to burst, fragment the magma, and resulted in an explosion. Phase 3 underwent efficient, open-system degassing; the volatiles in the magma were able to escape once the conduit was cleared from the previous explosion, therefore bubbles were not well preserved and microlites formed on the crystal surfaces during magma ascent through the conduit as a result of decompression-induced crystallization (Cashman and Blundy, 2000; Hammer and Rutherford, 2002; Couch et al., 2003). A dense, degassed lava dome was effused over a period of ~10 days, collapsed on 5 November,

and produced destructive PDCs that traveled 22 km down the volcanic edifice.

Lithium (Li) was building up in the melt prior to the 26 October explosion, however, this was not observed in crystals erupted on 5 November according to the SIMS depth profiles of these plagioclase phenocrysts (Genareau et al., 2014). Previous depth profile analyses have indicated that in andesite magmas, Li follows trends similar to H_2O, and an increase of Li in the melt indicates closed-system degassing, as it is not capable of leaving the system (Genareau et al., 2009; Genareau & Clarke, 2010). For the plagioclase crystals examined in this study, the increasing Li in the groundmass showed that the volatiles exsolving from the magma accumulated in the shallow system and contributed to the overpressure that caused the initial explosion.

The study of Toramaru (2006) used pumice samples from Plinian eruptions to calculate decompression rates based on their bubble number densities and properties of the magma under the assumption that nucleation was homogeneous, as is typical of Plinian events (Toramaru, 1995; Hurwitz and Navon, 1994; Massol and Koyaguchi, 2005). In this study, preserved vesicles on the plagioclase phenocryst crystal surfaces were used instead of pumice, which is a new method for calculating decompression rates. Merapi has characteristically erupted in Vulcanian style, suggesting a heterogeneous bubble nucleation regime due to crystal phases in the melt acting as preferential nucleation sites (Hurwitz and Navon, 1994; Fiege and Cichy, 2015). This could possibly explain why the BNDs calculated are comparable to Plinian pyroclastic BNDs. However, characteristics of the 2010 eruption suggest that the initial explosion was a single

decompression event causing bubbles to nucleate in a single stage. Merapi's magma was so crystal rich, the bubbles that formed would be in the interstitial melt directly next to the crystals, causing the nucleation to be essentially homogeneous even though the explosion was not Plinian. Although glass preserved on crystal surfaces provides a means to calculate BND, crystal surfaces may act as nucleation sites for bubbles in the magma (Hurwitz and Navon, 1994; Gardner and Denis, 2004; Gardner, 2007; Cluzel et al., 2008; Larsen, 2008) if bubble nucleation is heterogeneous, as is typical of Vulcanian explosions. If nucleation was heterogeneous, this could alter the measured BND values if bubbles are preferentially nucleating on the crystals rather than uniformly in the melt. However, the crystal-rich nature of the Merapi magma suggests that the interstitial melt between plagioclase phenocrysts is the only available location to nucleate bubbles, and thus the crystal surfaces may accurately reflect the nucleation dynamics at the point of fragmentation. Additionally, feldspars are less likely to nucleate bubbles than other mineral phases, such as magnetite (Mangan and Sisson, 2000; Gardner, 2007; Gualda and Ghiorso, 2007; Edmonds et al., 2014), suggesting that the plagioclase crystals used here do not preserve a higher concentration than other portions of the melt. Prior to the 26 October explosion, the system was sealed and pressurizing. The magma fragmented during the initial explosion of 2010 was unable to ascend or degas prior to decompression, and could only vesiculate at the onset of phase 2, suggesting that the magma experienced a single decompression, and thus, a homogenous nucleation regime.

Other studies of Vulcanian eruptions, such as Sakurajima, Japan, provide decompression

rates in the 10^4-10^5 Pa/s range (Miwa et al., 2009). For the Merapi 2010 explosion, it was hypothesized that the rates would be higher due to evidence of overpressure development (Genareau et al., 2014) in the magma prior to the sudden decompression event. The decompression rate meter confirmed this hypothesis providing higher rates (10^7- 10^8 Pa/s) than those determined for other Vulcanian eruptions. Toramaru (2006) also showed a correlation between column height and decompression rates. This study's results are similar to those seen at Plinian style eruptions that produce much larger eruptive column heights compared to the 2010 Merapi explosion. This indicates that the decompression rate during this eruption would be underestimated compared to similar Vulcanian-style events if the observed column height was used to infer the decompression rate.

Calculating decompression rates using bubbles preserved in the glass on crystal surfaces is a new method, as pumice lapilli clasts are typically utilized in such efforts. However, in many eruptive deposits (including those utilized here), such as pyroclastic surges and ash falls, lapilli-sized clasts may not be available for study. Consequently, examination of bubbles preserved on crystal surfaces may, in some cases, be the only means by which to calculate decompression rates of explosive eruptions. To test the validity of this method, Genareau and Cronin (*in preparation*) examined products of the 2014 Plinian eruption of Kelud (Java, Indonesia), a neighboring volcano of Merapi. This was a well-documented event that lasted ~6 hours, produced a column from 18-25 km in height, and resulted in widespread ash fall and numerous pyroclastic density currents that travelled down the edifice following collapse of both the pre-

existing dome and the Plinian column. Samples of these deposits were collected from numerous locations on the southwest flank and both pumice lapilli and phenocrysts within the ash-sized fraction were analyzed to determine the bubble number densities of pyroclasts. These measurements were used to calculate the decompression rate, which averages $6x10^7$ Pa/s, similar to other Plinian explosions, and the eruptive column height, which averages 25 km. This column height agrees well with observations of the eruption, and implies that vesicles preserved on phenocryst surfaces will provide a reliable source of data with which to determine explosive eruption parameters.

Decompression rates are an important parameter included in numerical modeling of explosive eruption dynamics (Alidibirov and Dingwell, 1996; Toramaru, 2006; Toramaru, 2014). Because decompression rates directly affect the height of the explosive eruption column, underestimation of these rates may result in smaller modeled column heights. This could result in an underestimation of the hazards resulting from explosive eruptions, posing significant implication for local communities at risk. Since Merapi usually experiences Vulcanian activity but has uncharacteristic explosive events every ~100 years, it's important to quantify the differences in eruption dynamics between the typical and unusual activity. Monitoring if and when degassing dynamics are transitioning from explosive activity to effusive activity could assist in future eruptions where this transition is observed, and help in better understanding sudden decompression events that may result in hazardous explosive activity.

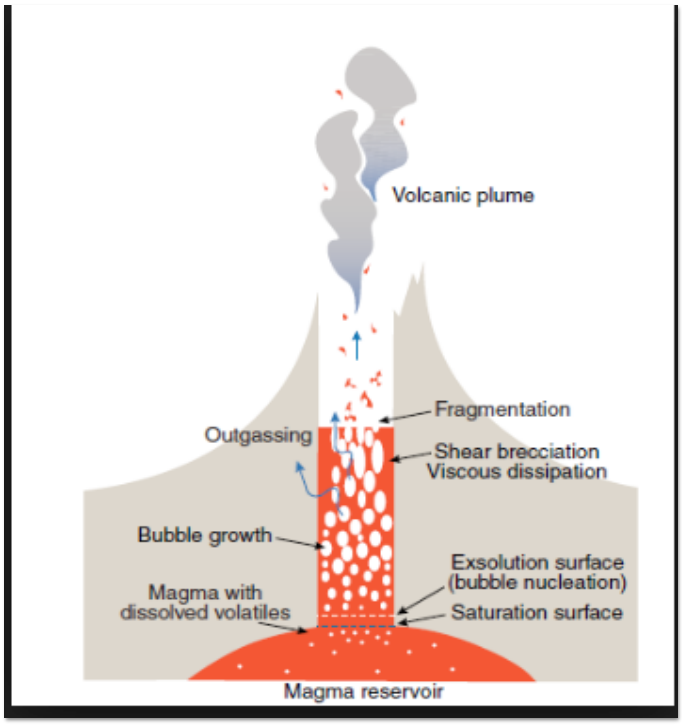

Figure 1: Illustration of intravolcanic processes. Magma containing dissolved volatiles, predominantly H_2O, CO_2, and SO_2, undergoes ascent-driven decompression. Gas bubbles are formed at the exsolution surface, but may escape through the conduit walls or the magma column. During explosive eruptions, bubble walls will rupture at the fragmentation surface causing released gases to expand rapidly. This causes the magma to change from a viscous melt to a gas flow with magma fragments.
(Gonnermann and Manga, 2007)

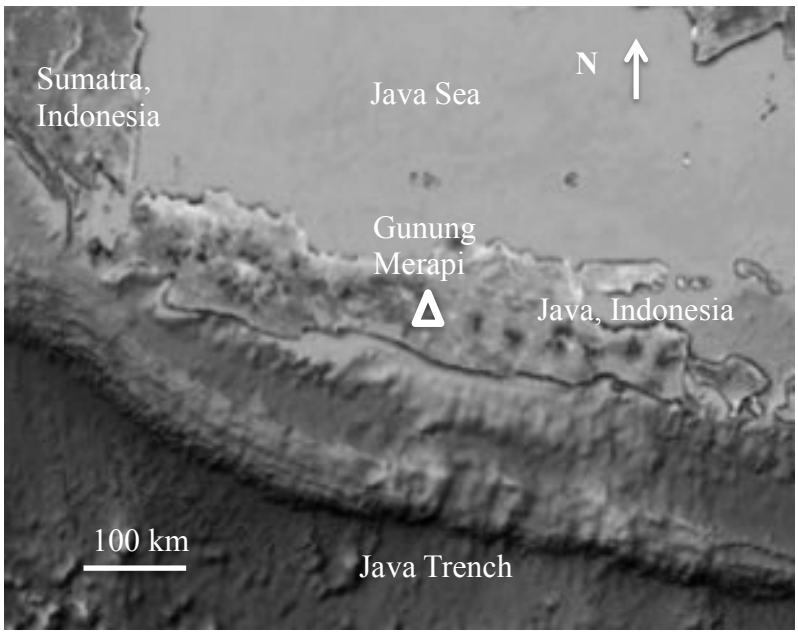

Figure 2: Location of Gunung Merapi volcano in Java, Indonesia.

Date	Stage of the eruption	Phase #
August 2010	Intrusion	1
Oct 26, 2010	Explosive	2
Nov 5, 2010	Effusive	3

Table 1: Listed dates with eruptive phase and phase number of the 2010 events as referred to in the text (Preece et al., 2014).

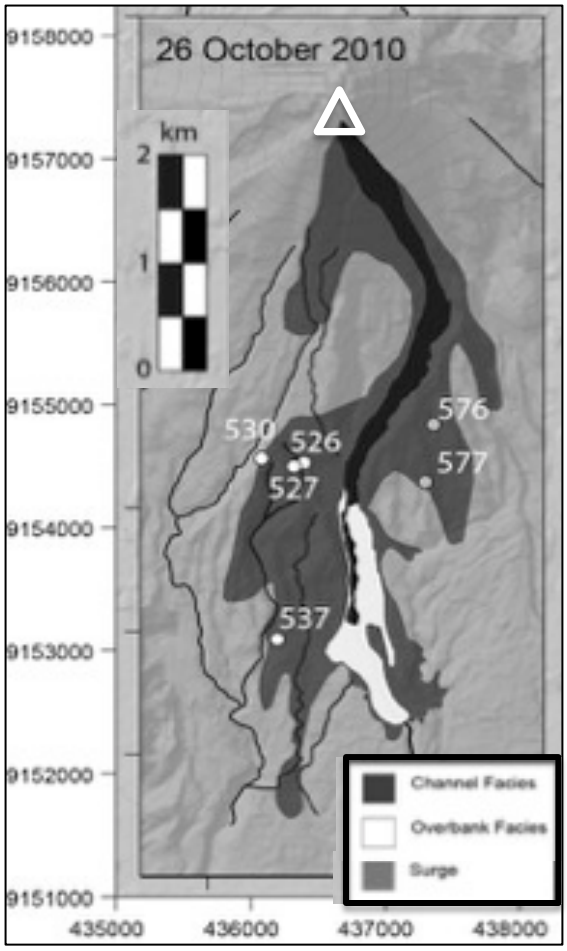

Figure 3: Location of samples taken from the pyroclastic density current deposits from phase 2. (Genareau et al., 2014).

Character	Value
a Constant (Toramaru, 2006)	$1x10^{15}$
Δ Interfacial tension (Toramaru, 2006)	0.298 (N/m)
D Diffusivity (Toramaru, 2006)	$2x10^{-11}$ m^2/s
Pw Saturation pressure (Costa et al., 2013)	$1x10^{8}$ Pa
T Temperature of melt (Costa et al., 2013)	1200 K
N Bubble number density (Toramaru, 2006)	Varied by crystal

Table 2: Variables used in the BND decompression rate meter and their values. Each one of these values (besides the constant provided by Toramaru 2006) is dependent upon melt properties.

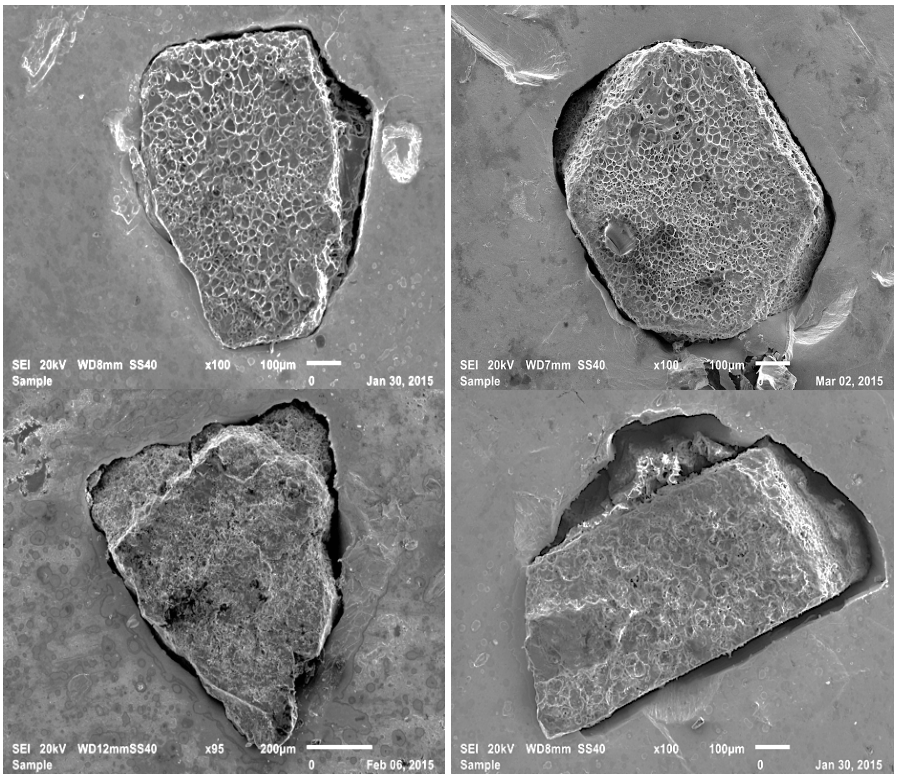

Figure 4: Top two images are SEM images of plagioclase crystals where the bubble walls are well defined. These crystals would be used for BND calculation, as opposed to the bottom crystals where there is little to no bubble wall formation and microlites present.

BND (m^{-3})	**Decompression rate (Pa/s)**
Range Minimum: $1.18x10^{13}$ Maximum: $1.5x10^{14}$	Range Minimum: $5.73x10^{7}$ Maximum: $2.64x10^{8}$
Average $3.84x10^{13}$	Average $1.13x10^{8}$

Table 3: Range and averages of calculated BNDs and decompression rates.

a	**D (m^2/s)**	**Δ (N/m)**	**P_w (Pa)**	**T (K)**	**N (m^{-3})**	**Decompression Rate (Pa/s)**
$1x10^{15}$	$2.00x10^{-11}$	0.298	$1.00x10^{8}$	1200	$1.29x10^{13}$	$6.08x10^{7}$
$1x10^{15}$	$2.00x10^{-11}$	0.298	$1.00x10^{8}$	1200	$2.00x10^{13}$	$8.14x10^{7}$
$1x10^{15}$	$2.00x10^{-11}$	0.298	$1.00x10^{8}$	1200	$2.63x10^{13}$	$9.77x10^{7}$
$1x10^{15}$	$2.00x10^{-11}$	0.298	$1.00x10^{8}$	1200	$3.82x10^{13}$	$1.25x10^{8}$
$1x10^{15}$	$2.00x10^{-11}$	0.298	$1.00x10^{8}$	1200	$4.44x10^{13}$	$1.39x10^{8}$
$1x10^{15}$	$2.00x10^{-11}$	0.298	$1.00x10^{8}$	1200	$6.02x10^{13}$	$1.7x10^{8}$
$1x10^{15}$	$2.00x10^{-11}$	0.298	$1.00x10^{8}$	1200	$1.50x10^{14}$	$3.12x10^{8}$
0% error	+ or – $0.5x10^{-11}$ m^2/s		+ or - 50 Pa	+ or - 100 K	5 % error	~6% error

Table 4: All of the values of the BND decompression rate meter (Pa/s) using the most reasonable melt parameters in the equation and the calculated errors. Explain what each variable is in the caption.

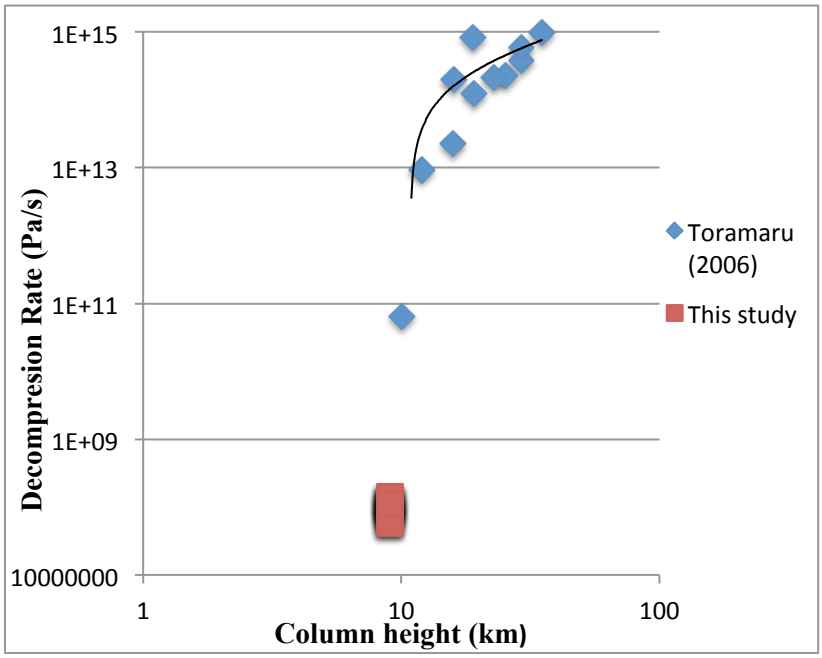

Figure 5: Toramaru (2006) Plinian data and Merapi's decompression rates plotted against column height.

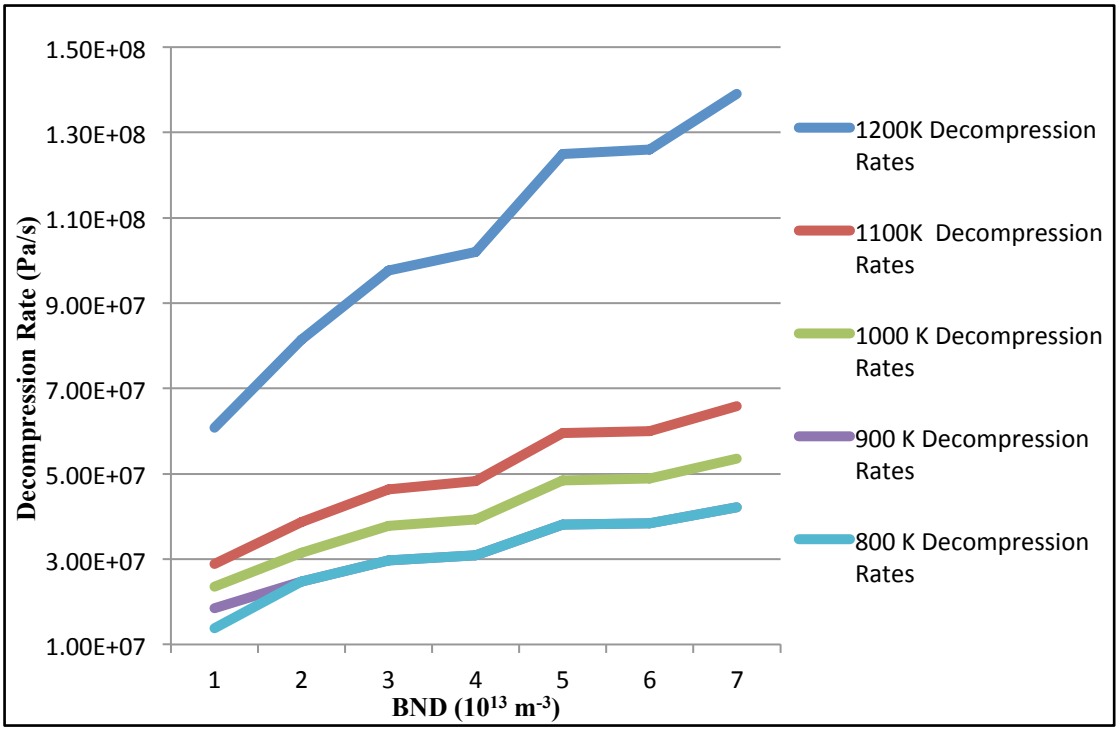

Figure 6: The original calculations were done at 1200 K. Lowering the temperature by 100 K lowered the rates slightly, but not nearly enough to be considered a factor in this eruption.

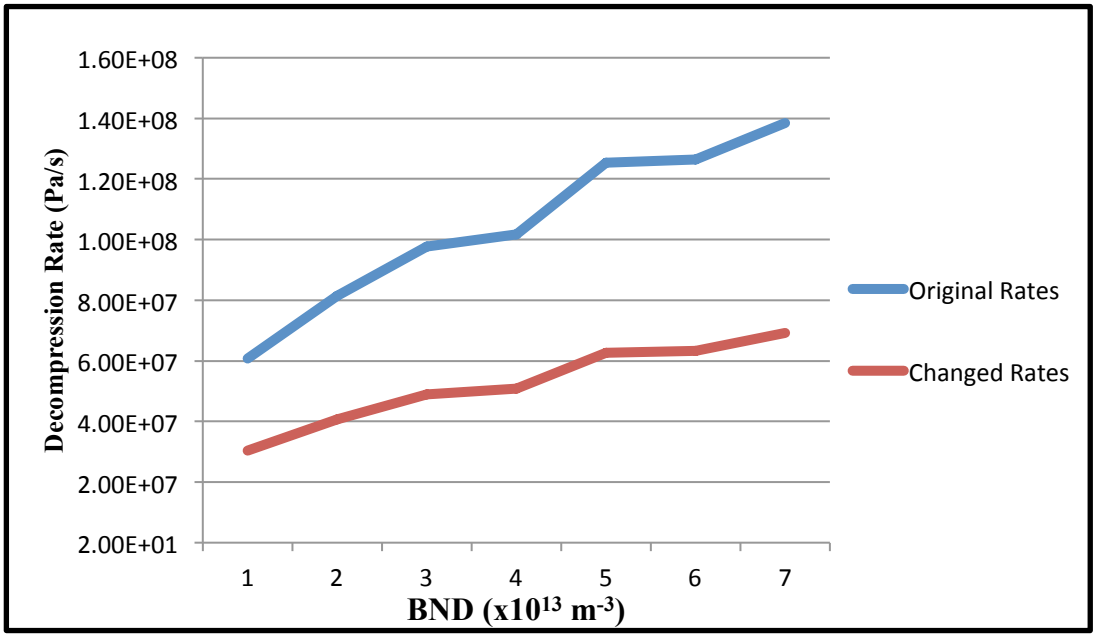

Figure 7: By raising the diffusivity from the original $2.00x10^{-11}$ to $1.0x10^{-11}$ m^2/s, there is a slight decrease in decompression rate, but not enough to be in comparable range to other Vulcanian style

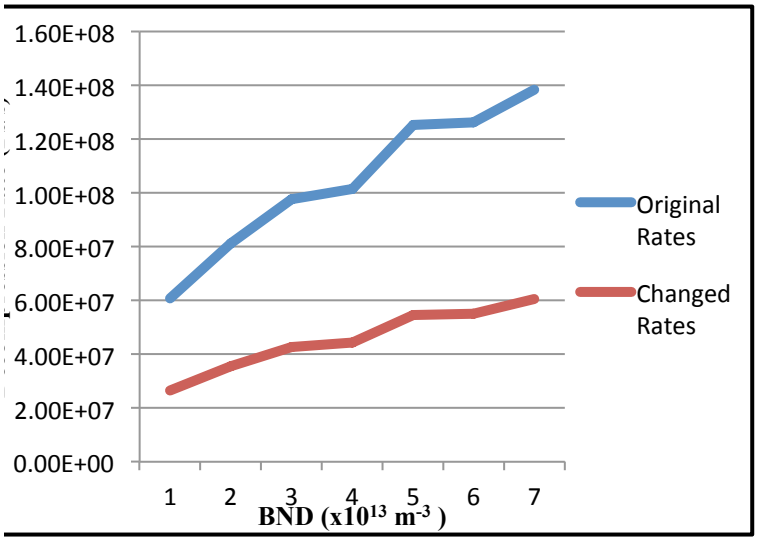

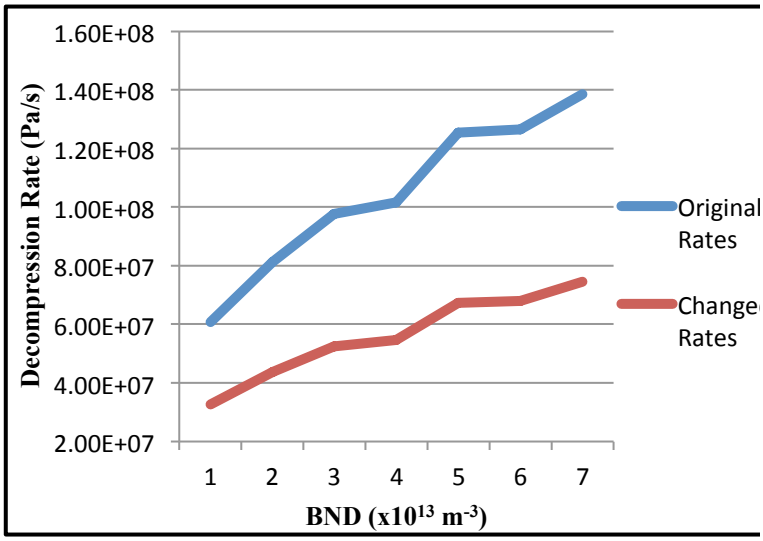

Figure 8: Plots showing the changes in saturation pressure show that there is very little to no change in decompression between our original saturation pressure and the increased numbers used for the sensitivity analysis. The top chart plots a small increase in saturation pressure ($1.1x10^8$ Pa) and the bottom chart shows a larger increase ($2.0x10^8$ Pa) Therefore, the saturation pressure would not be the cause in the calculated decompression rates.

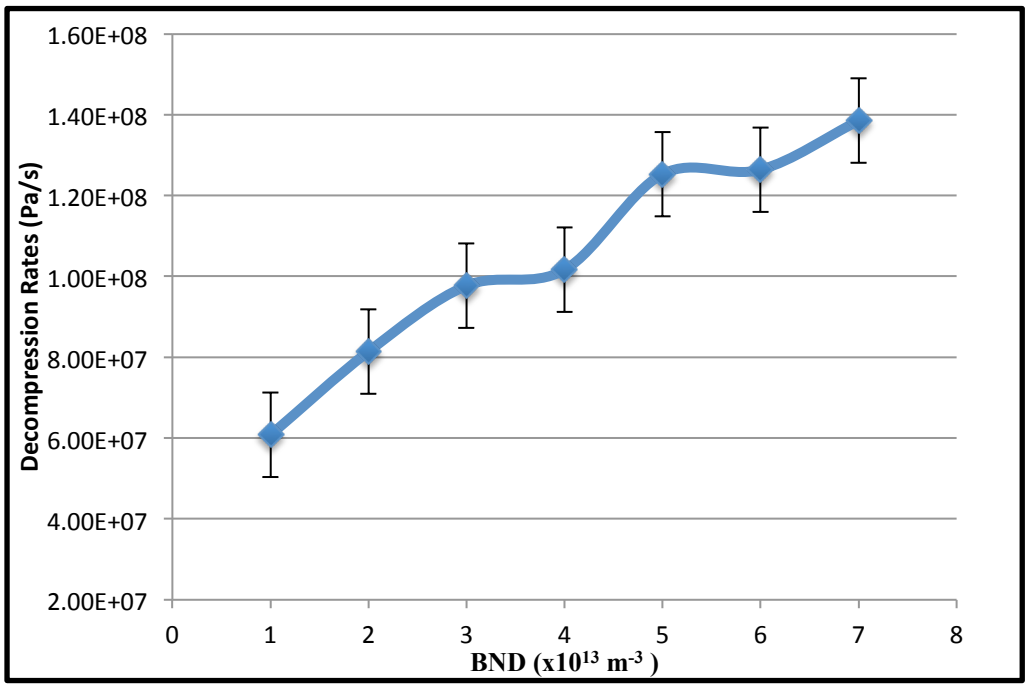

Figure 9: Decompression rate increases with increasing BND.

REFERENCES

Alidibirov, M, Dingwell, D.B. 1996. Magma fragmentation by rapid decompression. Nature 380,146–48

Blake, S. 1984. Volatile oversaturation during the evolution of silicic magma chambers as an eruption trigger. Journal of Geophysical Research.-Solid Earth, 89, 8237–44

Blundy, J. Cashman, K. 2001. Ascent-Driven crystallization of dacite magmas at Mount St Helens at Mount St Helens, 1980-1986. Contributions to Mineralogy and Petrology, 140, 631-650

Blundy, J., Cashman, K., 2005. Rapid decompression-driven crystallization recorded by melt inclusions from Mount St. Helens volcano. Geology, 33, 793-96

Camus, G., Gourgaud, A., Mossand-Berthommier, P-C., Vincent, P-M. 2010. Merapi (Central Java, Indonesia): an outline of the structural and mag- matological evolution, with a special emphasis to the major pyroclastic events. Journal of Volcanology and Geothermal Research, 100, 139–63

Cashman, K.V. 2004. Volatile Controls on Magma Ascent and Eruption. Geophysical Monograph, 19, 109-124.

Charbonnier, S.J. Gertisser, R. 2008. Field observations and surface characteristics of pristine block-and-ash flow deposits from the 2006 eruption of Merapi volcano, Java, Indonesia. Journal of Volcanology and Geothermal Research, 177, 971-982

Charbonnier, S.J., Gertisser, R. 2009. Numerical simulations of block-and-ash flows using the Titan2D flow model: examples from the 2006 eruption of Merapi Volcano, Bulletin of Volcanology, 71, 953-959

Charbonnier, S.J., Germa, A., Connor, C.B., Gertisser, R., Preece, K., Komoroski, J-C., Lavigne, F., Dixon, T., Connor, L. 2012. Evaluation of the impact of the 2010 pyroclastic density currents at Merapi volcano from high-resolution satellite imagery, field investigations and numerical simulations. Journal of Volcanology and Geothermal Research, http://dx.doi.org/10.1016/j.jvolgeores.2010.12.021

Cichy, S.B., Botcharnikov, R.E., Holtz, F., and Behrens, H. (2011) Vesiculation and microlite crystallization induced by decompression: A case study of the 1991–1995 Mt Unzen eruption (Japan). Journal of Petrology, 52, 1469–1492

Cluzel, N., Laporte, D., Provost, A., Kannewischer, I. 2008. Kinetics of heterogenous bubble nucleation in rhyolitic melts: implications for the number density of bubbles in volcanic conduits and for pumice textures. Contributions to Mineralogy and Petrology, 156, 745-763

Costa, F., Andreastuti, S., Bouvet de Maisonneuve, C., Pallister, J. 2013. Petrological insights into the storage conditions, and magmatic processes that yield the centennial 2010 Merapi explosive eruption. Journal of Volcanology and Geothermal Research, 261, 209-235

Couch, S., Sparks, R. S. J., & Carroll, M. R. (2003). The kinetics of degassing-induced crystallization at Soufriere Hills Volcano, Montserrat.Journal of Petrology, *44*(8), 1477-1502.

Cronin, S.J., Lube, G., Dayudi, D.S., Sumarti, S. Subrandiyo, S., Surono. 2013. Insights into the October-November 2010 Gunung Merapi eruption (Central Java, Indonesia) from the stratigraphy, volume and characteristics of its pyroclastic deposits. Journal of Volcanology and Geothermal Research, 261, 244-259, http://dx.doi.org/10.1016/j.jvolgeores.2013.01.005

Deegan, F.M., Troll, V.R., Freda, C., Misiti, V., Chadwick, J.P., McLeod, C.L., Davidson, J.P.2010. Magma-carbonate interaction processes and associated CO2 release at Merapi volcano, Indonesia: insights from experimental petrology. Journal of Petrology, 51, 1027– 51

Deegan, F.M, Troll, V.R., Freda, C., Misiti, V., Chadwick, J.P. 2011. Fast and furious: crustal CO2 release at Merapi volcano, Indonesia. Geology Today, 27, 63–64

Edmonds, M. and Brett, A. and Herd, R.A. and Humphreys, M.C.S. and Woods, A. 2014 'Magnetite-bubble aggregates at mixing interfaces in andesite magma bodies.', Geological Society of London special publications., 410 . p. 7.

Gardner, J.E., Denis, M.H. 2004. Heterogenous bubble nucleation of Fe-Ti oxide crystals in high-silica rhyolitic melts. Geochimica et Cosmochimica Acta, 68, 3587-3597

Gardner, J.E. 2007. Heterogenous bubble nucleation in highly viscous melts during instantaneous decompression from high pressure. Chemical Geology, 236, 1-12

Genareau, K., Clarke, A., B. 2010. In situ measurements of plagioclase growth using SIMS depth profiles of Li/Si: a means to acquire crystallization rates during short duration decompression events. American Mineralogists, 92, 1374-1382

Genareau, K., Cronin, S., Lube, G. 2014. Effects of volatile behaviour on dome collapse and resultant pyroclastic surge dynamics: Gunung Merapi 2010 eruption, Geological Society London Special Publications.

Gertisser, R., Keller, J. 2003. Temporal variations in magma composition at Merapi Volcano (Central Java, Indonesia): magmatic cycles during the past 2000 years of explosive activity. Journal of Volcanology and Geothermal Research, 123, 1-23

Gertisser, R., Charbonnier, S., Troll, V.R., Keller, J. 2011. Merapi (Java, Indonesia): anatomy of a killer volcano. Geology Today, 27, No. 2, 57-62

Gertisser, R., Charbonnier, S.J., Keller, J., Quidelleur, X. 2012. The geological evolution of Merapi volcano, Central Java, Indonesia. Bulletin of Volcanology, 74, 1213-1233

Gonnermann, H.M., Manga, M., 2007. The Fluid Mechanics Inside a Volcano. The Annual Review of Fluid Mechanics, 39, 321-56.

Gonnermann, H.M. 2015. Magma Fragmentation. Annual Review of Earth and Planetary Sciences, 43, 431-458

Gualda, G. A. R., Ghiorso, M. S. 2007. Magnetite scavenging and the buoyancy of bubbles in magmas. Part 2: Energetics of crystal-bubble attachment in magmas. Contributions to Mineralogy and Petrology, 154, 479–490.

Hamilton, W. 1979. Tectonics of the Indonesian region. US Geol Survey Prof Pap, 1078, 1-345

Hammer, J. E., Cashman, K. V., Voight, B. 2000. Magmatic processes revealed by textural and compositional trends in Merapi dome lavas. Journal of Volcanology and Geothermal Research, 100, 165–192.

Hammer, J. E., & Rutherford, M. J. 2002. An experimental study of the kinetics of decompression-induced crystallization in silicic melt. Journal of Geophysical Research: Solid Earth, 107(B1)

Holland, A.S.P, Watson, I.M., Phillips, J.C., Caricchi, L, Dalton, M.P. 2011. Degassing processes during lava dome growth: insights from Santiaguito lava dome, Guatemala. Journal of Geothermal Research, 202,153-166

Hurwtiz, S., Navon, O. 1994. Bubble nucleation in rhyolitic melts: Experiments at high pressure, temperature, and water content. Earth and Planetary Science Letters, 122, 267-280

Jaupart, C. 1996. Physical models of volcanic eruptions. Chemical Geology, 128, 217-227

Kennedy, B., Spieler, O., Scheu, B., Kueppers, U., Taddeucci, J., Dingwell, D.B., 2005. Conduit implosion during Vulcanian eruptions. Geology, 33, 581–584

Klug, C., Cashman, K.V.1994. Vesiculation of May 18 (1980) Mount St. Helens magma. Geology, 22, 468–472

Larsen, J.F. 2008. Heterogeneous bubble nucleation and disequilibrium H_2O exsolution in Vesuvius K-phonolite melts. Journal of Volcanology and Geothermal Research, 175, 278–288

Le Cloarec, M.F., Gauthier, P.J., 2003. Merapi volcano, Central Java, Indonesia: a case study of radionuclide behavior in volcanic gases and its implications for magma dynamics at andesite volcanoes. Journal of Geophysical Research,108, 2243. http://dx.doi.org/10.1029/2001JB001709.

Lube, G., Cronin, S.J., Thouret, J-C. Surono. 2011. Kinematic characteristics of pyroclastic density currents and controls on their avulsion from natural and engineered channels. Geological Society of America Bulletin, 123 (5–6), 1127–40

Manga, M., Stone, H.A. 1994. Interactions between bubbles in magmas and lavas: effects of bubble deformation. Journal of Volcanology and Geothermal Research, 63, 267–279

Mangan, M., Sisson, T. 2005. Evolution of melt-vapor surface tension in silicic volcanic systems: experiments with hydrous melts. Journal of Geophysical Research, 110, B01202.

Massol, H., Koyaguchi, T. 2005. The effect of magma flow on nucleation of gas bubbles in a volcanic conduit. Journal of Volcanology and Geothermal Research, 143, 69-88

Miwa, T., Tormaru, A., Iguchi, M. 2009. Correlations of volcanic ash texture with explosion earthquakes at vulcanian eruptions at Sakurajima volcano, Japan. Journal of Volcanology and Geothermal Research, 184, 473-486

Miwa, T., Geshi, N. 2012. Decompression rate of magma at fragmentation: Inference from broken crystals in pumice of vulcanian eruption. Journal of Volcanology and Geothermal Research, 227-28, 76-84

Nguyen CT, Gonnermann HM, Houghton BF. 2014. Explosive to effusive transition during the largest volcanic eruption of the 20th century (Novarupta 1912, Alaska). Geology, 42, 703–706

Parra, R. Bernard, B., Narvaez, D., Le Pennec, J.L., Hasselle, N., Folch, A. 2016. Eruption Source Parameters for forcasting ash dispersion and deposition from vulcanian eruptions at Tungurahua volcano: Insights from field data from the July 2013 eruption. Journal of Volcanology and Geothermal Research, 309, 1-13

Preece, K., Getisser, R., Barclay, J., Berlo, K., Herd, R.A. 2014. Pre-eruptive and syn-eruptive degassing and crystallization processes of the 2010 and 2006 eruptions of Merapi volcano, Indonesia. Contributions to Mineralogy and Petrolology 168:1061

Proussevitch, A.A., Sahagian, D.L., Kutolin, V.A. 1993. Stability of foams in silicate melts. Journal of Volcanology and Geothermal Research, 59, 161-178

Proussevitch, A.A., Sahagian, D.L. 1996. Dynamics of coupled diffusive and decompressive bubble growth in magmatic systems. Journal of Geophyiscal Research, 101, 17447-17455

Proussevitch, A.A., Sahagian, D.L. 1998. Dynamics and energetics of bubble growth in magmas: Analytical formulation and numerical modeling. Journal of Geophysical Research, 103, 18223-18251

Scandone, R., Cashman, K.V., Malone, S.D. 2007. Magma supply, magma ascent and the style of volcanic eruptions. Earth and Planetary Science Letters, 253, 513–529

Shinohara, H. 2008. Excess degassing from volcanoes and its role on eruptive and intrusive activity. Reviews in Geophysics, 46, 1–31

Sparks, R.S.J. 1978. The dynamics of bubble formation and growth in magmas: A review and analysis. Journal of Volcanology and Geothermal Research, 3, 1-37

Sparks, R.S.J., Jaupart, B.C., Mader, H.M., Phillips, J.C. 1994. Physical aspects of magma degassing; 1, Experimental and theoretical constraints on vesiculation. Review in Mineralogy and Geochemistry, 30, 413-445

Sparks, R.S.J. 2003. Forecasting volcanic eruptions. Earth and Planetary Science Letters, 210, 1-15

Sparks, R.S.J., Huppert, H.E., Turner, J.S. 1984. The fluid-dynamics of evolving magma chambers. Philosophical Transitions of the Royal Society A: Mathematical, Physical and Engineering Sciences, 310, 511-32

Surono, M., Jousset, P., Pallister, J., Boichu, M., Buongiorno, M.F. 2012. The 2010 explosive eruption of Java's Merapi volcano - a '100-year' event. Journal of Volcanology and Geothermal Research, Elsevier, 241-242, 121-35. <10.1016/j.jvolgeores.2012.06.018>.

Tormaru, A. 1989. Vesiculation process and bubble size distributions in ascending magmas with constant velocities. Journal of Geophysical Research, 94, 17523-17542

Tormaru, A. 1995. Numerical study of nucleation and growth of bubbles in viscous magmas. Journal of Geophysical Research, 100, 1913-1931

Toramaru, A. 2006. BND (bubble number density) decompression rate meter for explosive volcanic eruptions. Journal of Volcanology and Geothermal Research, 154, 303-16

Toramaru, A.2014. On the second nucleation of bubbles in magmas under sudden decompression. Earth and Planetary Science Letters, 404, 190-99

Varley, N., Arambula-Mendoza, R., Reyes-Davila, G., Sanderson, R., Stevenson, J. 2010. Generation of Vulcanian activity and long-period seismicity at Volcan de Colima, Mexico. Journal of Volcanology and Geothermal Research, 198, 1-2, 45-56.

Voight, B. Constantine, E.K., Siswowidjoyo, S., Torley, R. 2000. Historical eruptions of Merapi volcano, Central Java, Indonesia, 1768-1998. Journal of Volcanology and Geothermal Research, 100, 69-138

Wallace, P.J., Anderson Jr., A.T., Davis, A.M., 1995. Quantification of pre-eruptive exsolved gas contents in silicic magmas. Nature, 337, 612-16

Walter, T.R., Wang, R., Zimmer, M., Grosser, H., Lühr, Ratdomopurbo, B.A. 2007. Volcanic activity influenced by tectonic earthquakes: static and dynamic stress triggering at Mt. Merapi. Geophysical Research Letters, v.34